ORIGINAL RESEARCH

Concomitant Obesity and Metabolic Syndrome Add to the Atrial Arrhythmogenic Phenotype in Male Hypertensive Rats

Mathias Hohl, PhD; Dennis H. Lau, MBBS, PhD; Andreas Müller, PhD; Adrian D. Elliott, PhD; Benedikt Linz, MSc; Rajiv Mahajan, MD, PhD; Jeroen M. L. Hendriks, PhD; Michael Böhm, MD; Ulrich Schotten, MD, PhD; Prashanthan Sanders, MBBS, PhD; Dominik Linz, MD, PhD

***Background*—**Besides hypertension, obesity and the metabolic syndrome have recently emerged as risk factors for atrial fibrillation. This study sought to delineate the development of an arrhythmogenic substrate for atrial fibrillation in hypertension with and without concomitant obesity and metabolic syndrome.

***Methods and Results*—**We compared obese spontaneously hypertensive rats (SHR-obese, n=7–10) with lean hypertensive controls (SHR-lean, n=7–10) and normotensive rats (n=7–10). Left atrial emptying function (MRI) and electrophysiological parameters were characterized before the hearts were harvested for histological and biochemical analyses. At the age of 38 weeks, SHR-obese, but not SHR-lean, showed increased body weight and impaired glucose tolerance together with dyslipidemia compared with normotensive rats. Mean blood pressure was similarly increased in SHR-lean and SHR-obese when compared with normotensive rats (178±9 and 180±8 mm Hg [not significant] versus 118±5 mm Hg, $P<0.01$ for both), but left ventricular end-diastolic pressure was more increased in SHR-obese than in SHR-lean. Impairment of left atrial emptying function, increase in total atrial activation time, and conduction heterogeneity, as well as prolongation of inducible atrial fibrillation durations, were more pronounced in SHR-obese as compared with SHR-lean. Histological and biochemical examinations revealed enhanced triglycerides and more pronounced fibrosis in the left atrium of SHR-obese. Besides increased expression of profibrotic markers in SHR-lean and SHR-obese, the profibrotic extracellular matrix protein osteopontin was highly upregulated only in SHR-obese.

***Conclusions*—**In addition to hypertension alone, concomitant obesity and metabolic syndrome add to the atrial arrhythmogenic phenotype by impaired left atrial emptying function, local conduction abnormalities, interstitial atrial fibrosis formation, and increased propensity for atrial fibrillation. **(*J Am Heart Assoc*. 2017;6:e006717. DOI: 10.1161/JAHA.117.006717.)**

Key Words: atrial fibrillation • hypertension • metabolic syndrome • obesity

Atrial fibrillation (AF) is a progressive rhythm disorder and over the course of time, many patients progress from paroxysmal to more sustained forms of the arrhythmia.[1,2] Recent data suggest that both the type of AF and progression of the underlying disease are determined by the number of concomitant risk factors.[3] The most prevalent risk factors in patients with AF are hypertension, obesity, and metabolic syndrome (MetS).[3] MetS has been shown to amplify cardiovascular risk independent of the effect of several traditional cardiovascular risk factors in patients with hypertension.[4] Obesity and the MetS frequently coexist in patients with hypertension and increase the risk of heart failure with preserved ejection fraction and diastolic dysfunction.[5] Previous studies demonstrated the development of an atrial arrhythmogenic substrate in animal models for hypertension[6–9] as well as for diabetes mellitus and obesity.[10,11] However, uncertainty exists as to how concomitant obesity and MetS add to the atrial arrhythmogenic phenotype in the context of hypertension.

Structural and electrophysiological remodeling processes in the atrium contribute to the progression of AF.[1] Next to cardiomyocyte hypertrophy, extracellular fibrosis formation in the atrium was reported to impact the occurrence and maintenance of AF by impairment of intra-atrial and interatrial

From the Klinik für Innere Medizin III, Universitätsklinikum des Saarlandes, Homburg/Saar, Germany (M.H., B.L., M.B., D.L.); Centre for Heart Rhythm Disorders, South Australian Health and Medical Research Institute, Royal Adelaide Hospital, University of Adelaide, Australia (D.H.L., A.D.E., R.M., J.M.L.H., P.S., D.L.); Klinik für Diagnostische und Interventionelle Radiologie, Universitätsklinikum des Saarlandes, Homburg/Saar, Germany (A.M.); Cardiovascular Research Institute Maastricht (CARIM), University Maastricht, Maastricht, The Netherlands (U.S.).

Correspondence to: Dominik Linz, MD, PhD, Department of Cardiology, Centre for Heart Rhythm Disorders, Royal Adelaide Hospital, Adelaide 5000, Australia. E-mail: dominik.linz@adelaide.edu.au

Received May 19, 2017; accepted July 24, 2017.

Clinical Perspective

What Is New?

- Concomitant obesity and metabolic syndrome add to the atrial arrhythmogenic phenotype by impaired atrial emptying function, local conduction abnormalities, interstitial atrial fibrosis formation, and increased propensity for atrial fibrillation.

What Are the Clinical Implications?

- Assessment of concomitant risk factors such as obesity and metabolic syndrome should be part of the routine workup in patients with hypertension.
- Aggressive risk factor and weight management should be considered to maximize the prevention of the development of an atrial arrhythmogenic remodeling process and to maintain sinus rhythm.
- The proinflammatory adhesion protein osteopontin is upregulated in hypertension with concomitant obesity and may represent a pharmacological target to prevent atrial structural remodeling.

electrical conduction propagation.[12,13] The profibrotic cytokines transforming growth factor beta (TGF-β) and osteopontin (OPN) are upregulated in MetS[10,11,14] and play pivotal roles in the development of cardiac fibrosis and remodeling.[15,16] Elevated blood levels of TGF-β[17] as well as OPN[18] have been shown to be associated with increased recurrence of AF after catheter ablation.

This study sought to examine the development of an electrophysiological and structural substrate for AF in hypertension with and without concomitant obesity and MetS. An obese spontaneously hypertensive rat model, in which multiple abnormal phenotypes including hypertension, obesity, hyperinsulinemia, and hyperlipidemia are expressed,[19–22] was used and compared with lean spontaneously hypertensive rats (SHR-lean) and normotensive controls.

Materials and Methods

Animals

Male obese spontaneously hypertensive rats (SHR-obese, n=14), their control littermates (SHR-lean, n=14), and male normotensive Sprague-Dawley rats (controls, n=14) were purchased from Charles River Germany GmbH at an age of 10 weeks. As SHR-obese were developed from a cross between an SHR-lean and a normotensive Sprague-Dawley rat, we used Sprague-Dawley as the correct normotensive control for SHR-obese. We are aware that Sprague-Dawley rats do not represent the most appropriate control for the SHR-lean and some of the comparisons in this study need to be seen with precaution. The animals were housed individually in standard cages and received a standard chow diet (standard diet #1320, Altromin) and tap water ad libitum. The animal experiments were conducted in accordance with the National Institutes of Health Guide for the Care and Use of Laboratory Animals and with the welfare guidelines and the German law for the protection of animals. The procedures followed were in accordance with institutional guidelines. The study was approved by the regional animal ethics commission in Darmstadt, Germany.

Study Design

Our study aimed to investigate the development of an arrhythmogenic substrate for AF comparing the influence of hypertension alone with the additive effect of concomitant obesity and MetS.

At 22 weeks of age, implantation of telemetric sensors was performed under isoflurane anesthesia in 7 animals per group. After a postoperative recovery period of 2 weeks, telemetric monitoring was performed for ≈16 weeks. At the age of 38 weeks, blood was obtained from the retro-orbital plexus under light anesthesia (3.5% isoflurane). Fasting blood glucose, glycated hemoglobin, triglyceride, and cholesterol levels were measured using standard kits (Cobas Integra, Roche Diagnostics). The concentration of OPN was determined in plasma using a radio immunoassay (Phoenix Pharmaceuticals Inc). At 38 weeks of age, left atrial (LA) function was assessed by cardiac MRI. One week later, invasive left ventricular (LV) pressure measurements and electrophysiological studies were performed, after which the animals were euthanized and atrial tissue was further processed for immunohistological and biochemical analyses.

Telemetry

Implantation of telemetric sensors was performed under isoflurane anesthesia in 7 animals per group. An abdominal incision was made through the skin and underlying muscle wall along the ventral midline, and the descending aorta was carefully isolated by blunt dissection. A ligature (2-0 braided silk, Ethicon) was inserted between the aorta and the vena cava to allow insertion of the catheter tip of the transmitter (TL11M2-C50-PXT PMP, Data Sciences International) into the aorta after puncture with a small needle. At the puncture site, a drop of surgical glue (3 MVetbond, Tissue Adhesive) was applied to secure the catheter. Furthermore, the transmitter was secured in the abdomen by suture to the muscle wall. After 2 weeks of recovery, blood pressures were acquired and heart rates were derived from the beat-to-beat signal for ≈16 weeks at a sampling rate of 500 Hz, and data were stored as 2-minute averages throughout the 16 weeks. At 38 weeks of age, the mean value of all measurements during a period of 24 hours

was used to determine the mean 24-hour arterial blood pressure. Twenty-four-hour arterial blood pressure was used for statistical analysis and data presentation. For analysis and data plotting, the vendor software (Dataquest A.R.T., version 4.0) was used. Because of the implanted telemetry catheter, these animals could not be used for MRI studies.

Magnetic Resonance Imaging

At the age of 38 weeks, cardiac LA function was assessed by cardiac MRI in an additional 7 animals per group without implanted telemetric sensors (rats were anesthetized with 1.5–2.5% isoflurane). All scans were acquired with a 7-T MRI scanner (Bio Spec 70/30). Multislice short-axis cine imaging was performed from the upper LA roof to the apex with a slice thickness of 1.2 mm and an interslice gap of 0 mm. Orthogonal long-axis cine imaging of the left atrium was acquired. LA boundaries were obtained in each short-axis image. The LA volumes were then determined by Simpson's rule. LA area was manually encircled. The point of insertion of the mitral valve leaflets was taken as the atrioventricular border. Pulmonary veins were excluded at their ostia and the LA appendage was excluded at its base. All dimensions were measured throughout the cardiac cycle. The cardiac cycle was divided into 10 equal phases with an interphase time difference of the spontaneous cycle length/10. The MRI images of all left atriums were analyzed by the same investigator blinded to animal groupings.

Minimal LA (LAmin) and maximal LA volume (LAmax) and their difference (cyclical change volume) were determined from the LA volume/time curves. The minimal volume at the end of rapid passive emptying (LAre) and the volume before active emptying (LApc) were determined from the volume time curves as described elsewhere.[23] LA emptying function parameters (total percent emptying ((LAmax−LAmin)/LAmax), active percent emptying ((LApc−LAmin)/LApc), and passive percent emptying ((LAmax−LAre)/LAmax)) were computed.[23] LA volume/body weight ratio (LA volume index) was determined to normalize LA dimensions.

To measure regional LA wall motion, a typical horizontal long-axis 4-chamber image was used for analysis. Regional wall motion in the radial dimension was measured from an arbitrary central reference point in the center of the left atrium to the midpoint of each of four segments: the annular chord, the posterior chord, the septal chord, and the lateral chord.[24]

Invasive Measurement of End-Diastolic LV Pressure

At the age of 38 weeks, all animals were anaesthetized with thiopental (Narcoren, 100 mg/kg i.p., Merial), intubated, and lungs artificially ventilated. End-diastolic LV pressure was assessed using a Millar Tip catheter (Millar Instruments Inc), which was introduced from the right carotid artery and advanced into the LV cavity. Data were digitized with a sampling rate of 1000 Hz and recorded on a PC using specialized software (HEM, Notocord).

Electrophysiological Studies

Surface ECG (lead II) was recorded via subcutaneous needle electrodes. After completion of the invasive measurement of end-diastolic LV pressure, a custom-made mapping electrode with 4*5 unipolar electrodes (1.0-mm interelectrode distance) was placed on the LA free wall to analyze atrial conduction. Unipolar signals were recorded using a custom-made channel mapping amplifier (filtering bandwidth 0.1–408 Hz, sampling rate 1.0 kHz, A/D resolution 16 bits). Unipolar pacing was performed from the surface of the left atrium (pulse width of 1 ms at twice the diastolic threshold, cycle length: 150 ms). Maps from 5 consecutive beats were analyzed. Local activation times were identified by maximum negative dV/dt in each unipolar ECG. Local activation time differences were calculated between neighboring electrodes (conduction times). Conduction times of $\geq$3 ms (equivalent to conduction velocities $\leq$33 cm/s) were considered as being prolonged.[25] Total atrial activation time was defined as the time difference between the right atrial activation time, visualized by a custom-made multiple action potential catheter (Franz-like electrode) next to the pacing electrode, and the latest LA activation time recorded by the mapping electrode during right atrial pacing (cycle length: 150 ms). Atrial effective refractory period (AERP) was measured at a basic cycle length of 150 ms at the free wall of the left atrium. The mean of 3 AERP measurements was used for analysis. Susceptibility to AF was tested using repetitive 1-second bursts of stimuli (cycle length: 10 ms). When atrial ECGs showed a rapid atrial rate, cycle length <70 ms, and duration >5 beats, AF was diagnosed. The duration of the longest of 3 induced subsequent episodes of AF was taken as inducible AF duration.

Atrial Histology

At the conclusion of the hemodynamic and electrophysiological assessments, hearts were rapidly removed, trimmed free from noncardiac tissues, and weighed. Thereafter, the separated left atrium was fixed in buffered 4% formaldehyde for 24 hours and embedded in paraffin for histological evaluation. Tissue sections of 5 μm were fixed at 56°C overnight, deparaffinized, rehydrated, and stained with hematoxylin and eosin to determine cardiomyocyte diameter as a measure of cardiomyocyte hypertrophy and myocyte-myocyte distances within bundles as a measure of enhanced extracellular LA matrix formation and endomysial fibrosis formation.[11] To visualize total tissue

fibrosis amount, the sections were stained with Picro-Sirius Red. The percentage of the left atrium consisting of interstitial collagen was calculated as the ratio of the Picro-Sirius Red positively stained area over total LA tissue area, excluding blood vessels and the epicardial and endocardial plane, using ImageJ 1.37a (National Institutes of Health). Fibrosis was quantified on 3 sections per atrium (6–8 fields per section).

Atrial Triglyceride Content

Intramyocardial triglyceride content was determined by a triglyceride colorimetric assay kit (Cayman Chemicals) according to the supplier's instruction. Protein concentration in the respective aliquot was determined using the Bradford protein assay kit (#500-0113, #500-0114, Bio-Rad Laboratories).

Gene Expression Analyses

Gene expression analysis was performed by real-time polymerase chain reaction. Total RNA was extracted from whole left atrium by homogenizing in RLT buffer and by using RNeasy Mini columns (Qiagen). Genomic DNA impurities were removed by DNase treatment (DNA Removal Kit, Ambion), and cDNA was synthesized by reverse transcription (Life Science Technologies). Quantitative real-time polymerase chain reaction was performed using Taqman primers on an ABI Prism 7500 Sequence Detector (Applied Biosystems) and c(t) values obtained by using a respective software (SDS version 1.9). C(t) values were normalized to corresponding GAPDH controls. The ΔCt was used for statistical analysis and $2^{-\Delta\Delta Ct}$ standardized to the control group was used for data presentation. Probes used to amplify the transcripts were as follows (purchased by Applied Biosystems): GAPDH (Rn99999916_s1), OPN (Spp1) (Rn00681031_m1), TGF-β1 (Rn00572010_m1), Col1a1 (Rn01463848_m1), connective tissue growth factor (Rn01537279_g1), and sarcoplasmic reticulum calcium ATPase type 2A (ATP2a2 Rn00568762_m1).

Statistical Analysis

Statistical analysis was performed using Prism software (GraphPad). The data are expressed as means±SEM. Statistical significance was assessed by ANOVA, followed by Bonferroni post-test. *P* values of <0.05 were considered statistically significant.

Results

Metabolic and Hemodynamic Parameters

Body weight index in SHR-obese (body weight normalized on individual tibia length/tibia length of SHR ratio) was significantly higher compared with SHR-lean and controls (Figure 1A). Fasting serum insulin levels were significantly elevated in SHR-obese compared with SHR-lean and controls. However, SHR-obese did not show fasting hyperglycemia and glycated hemoglobin was not increased. SHR-obese showed increased triglyceride and cholesterol blood levels compared with SHR-lean and controls. At 38 weeks of age, telemetry analysis in 7 animals per group revealed a similar increase in mean arterial blood pressure in SHR-lean and SHR-obese when compared with controls (Figure 2A). Heart rate was significantly lower in SHR-lean and SHR-obese compared with controls (Figure 2B). LV end-diastolic pressure was more increased in SHR-obese than in SHR-lean (Figure 2C). LA dimensions, determined by LA volume/body weight indices, were similarly increased in SHR-obese and SHR-lean compared with controls (Figure 2D). A more intensive metabolic and ventricular hemodynamic characterization of the SHR-obese and SHR-lean models has been previously published.[20]

LA Emptying Function

LA emptying function parameters are shown in Figure 3. Global LA emptying function, as assessed by total percent emptying (Figure 3A), active percent emptying, and passive percent emptying (Figure 3B and 3C) were not changed in SHR-lean when compared with controls. SHR-obese displayed a significant reduction of total, passive, and active percent emptying compared with both controls and SHR-lean.

To determine regional LA wall motion, we measured radial fractional shortening of the left atrium (Figure 3D). In SHR-obese, radial fractional shortening was significantly diminished in the lateral and posterior segments of the left atrium compared with control rats ($P<0.01$). The remaining segments displayed normal radial motion. SHR-lean rats showed a trend towards reduced radial fractional shortening of the left atrium in the annular ($P=0.07$) and posterior ($P=0.10$) segment, although these changes did not achieve statistical significance.

Atrial Electrophysiology

Short episodes of AF could be induced in all rats investigated in our study. Increase in total atrial activation time (Figure 4A) and percentage of regions with slow conduction during rapid pacing (Figure 4B) was significantly more pronounced in SHR-obese than in SHR-lean when compared with controls. AERP, however, was similarly prolonged in SHR-obese and SHR-lean (Figure 4C) as compared with controls. The median duration of inducible AF was prolonged in SHR-lean and SHR-obese compared with controls. AF episodes were longer in SHR-obese compared with controls and SHR-lean (Figure 4D).

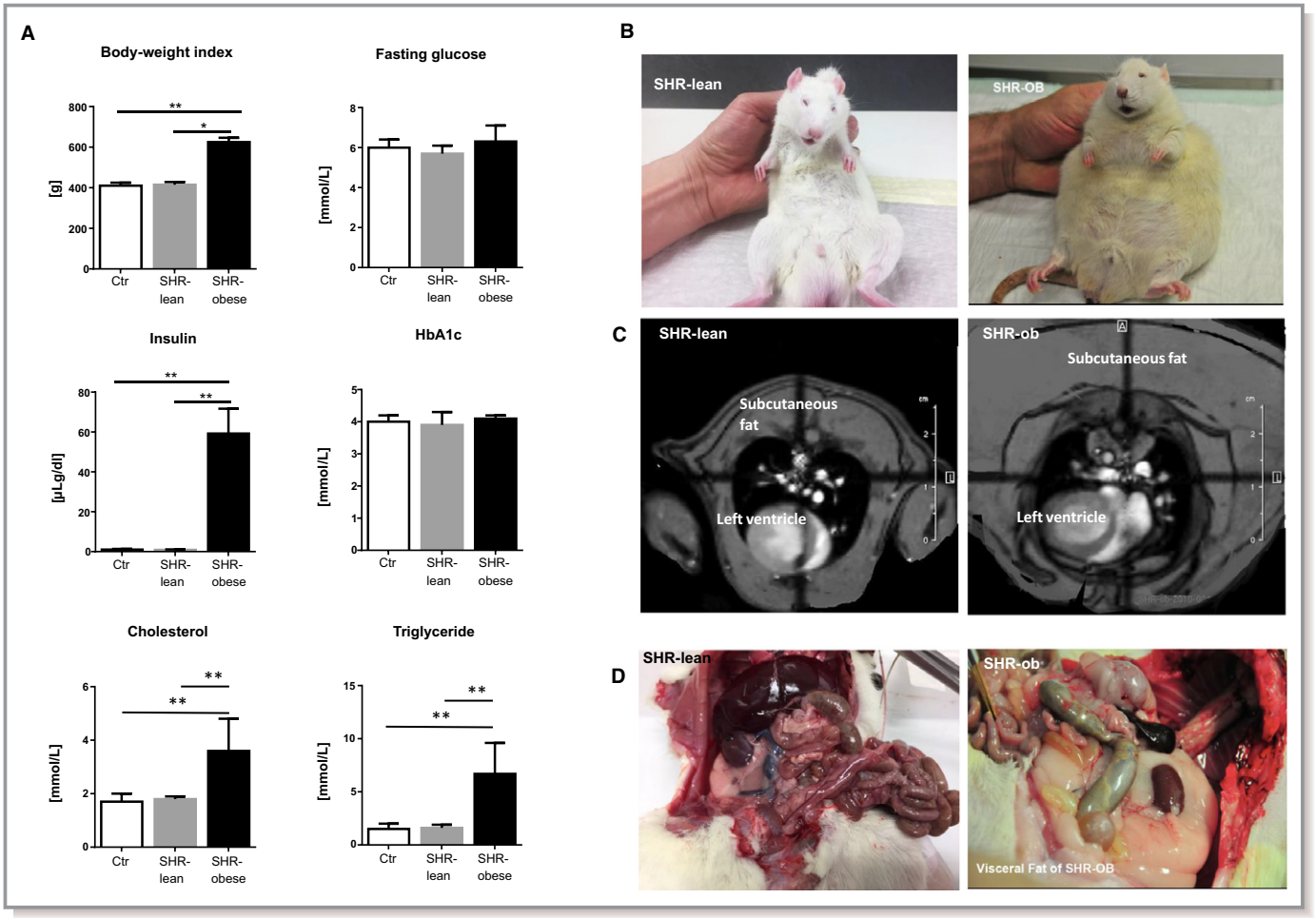

Figure 1. Metabolic parameters and phenotypes of lean spontaneously hypertensive rats (SHR-lean) and obese spontaneously hypertensive rats (SHR-obese). A, Quantification of body weight index of controls (Ctr; n=10), SHR-lean (n=10), and SHR-obese (n=10). Levels of fasting serum glucose, insulin, glycated hemoglobin (HbA1c), cholesterol, and triglyceride. B, Representative pictures of SHR-lean and SHR-obese for comparison. C, Representative pictures of magnetic resonance imaging scans showing subcutaneous fat in SHR-lean and SHR-obese. D, Representative pictures of visceral fat in the abdomen of SHR-lean and SHR-obese. All values are mean±SEM. **P*<0.05, ***P*<0.01.

LA Structural Remodeling and Gene Expression Analyses

Total LA tissue fibrosis was increased in SHR-obese, but not in SHR-lean, as compared with controls (Figure 5A and 5B). Myocyte-myocyte distances within bundles as a measure of enhanced extracellular LA matrix and endomysial fibrosis formation, and LA myocyte diameters as a measure of cardiomyocyte hypertrophy, were enlarged in SHR-obese and SHR-lean (Figure 5A and 5C) as compared with controls. Furthermore, the increase in endomysial fibrosis formation and cardiomyocyte hypertrophy was more pronounced in SHR-obese than in SHR-lean (Figure 5B and 5C). Expression of TGF-β was upregulated in both SHR-obese and SHR-lean, while mRNA levels of connective tissue growth factor and collagen 1a were higher in SHR-obese compared with SHR-lean (Table). A significant 36% decrease in gene expression of the calcium-handling protein sarcoplasmic reticulum calcium ATPase type 2A was observed in SHR-obese, but not in SHR-lean, when compared with controls (Table). LA gene expression of the profibrotic extracellular matrix protein OPN was highly upregulated only in SHR-obese (Figure 5D). OPN plasma concentration was exclusively increased in SHR-obese compared with both SHR-lean and controls (16.1±1.4 ng/mL in SHR-obese versus 7.4±0.4 ng/mL in SHR-lean and 6.2±0.5 ng/mL in controls, $P<0.01$ for both) (Figure 5D). In the LA tissue, intramyocardial triglyceride content was significantly higher in SHR-obese compared with SHR-lean and controls (23.2±5.1 versus 11.6±1.9 and 10.4±2.1 nmol TG/mg protein, respectively; Figure 5E). Despite enhanced intramyocardial triglyceride content, visceral and subcutaneous adipose tissue in SHR-obese, increased interstitial LA fatty dispositions, and epicardial fat depots were not detected in LA histological stainings or macroscopically or in MRI scans.

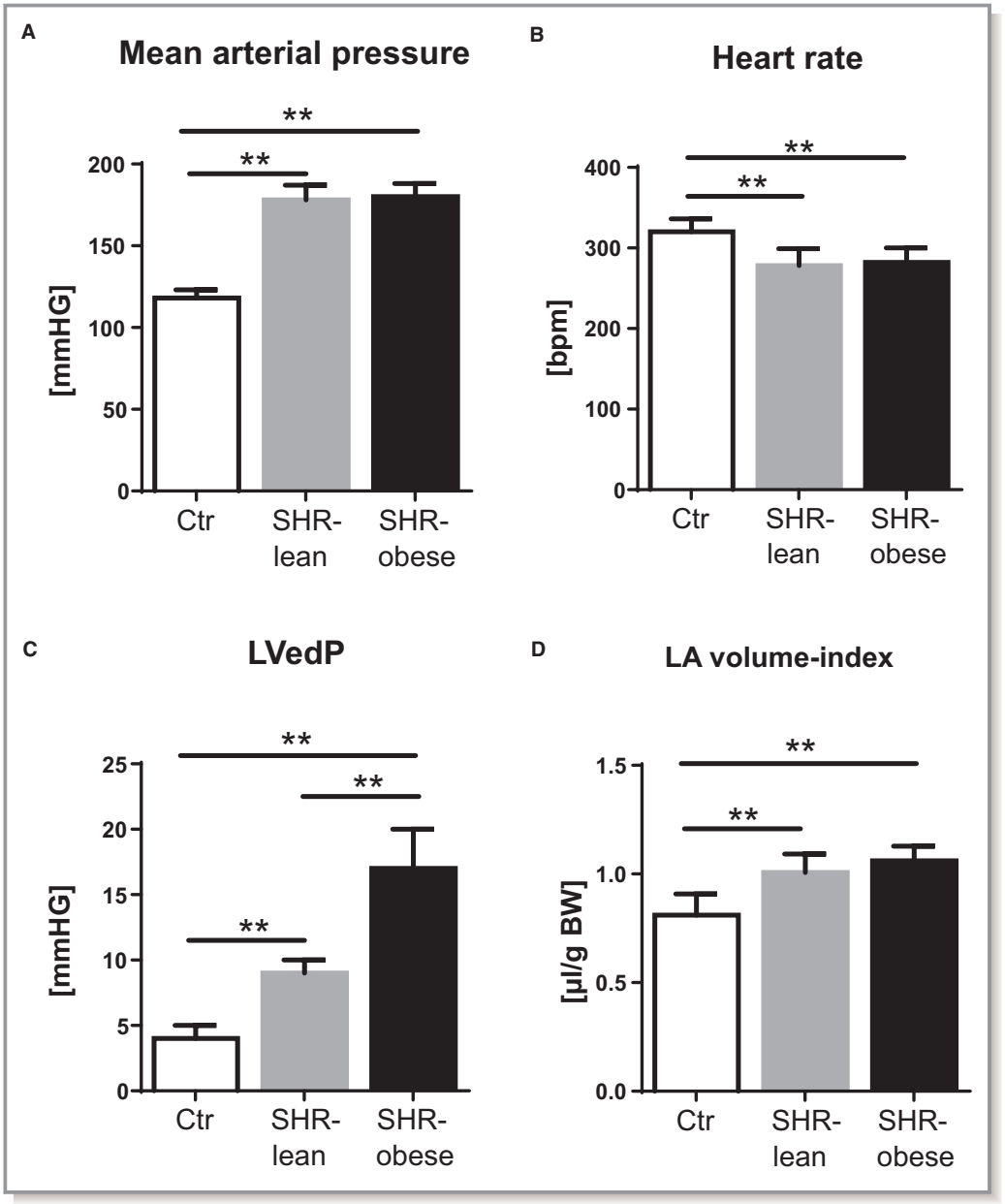

Figure 2. Hemodynamic parameters of lean spontaneously hypertensive rats (SHR-lean) and obese spontaneously hypertensive rats (SHR-obese). Quantification of (A) mean arterial pressure and (B) heart rate measured by catheter-based telemetry (n=7) per group. C, Assessment of left ventricular end-diastolic pressure (LVedP) measured by Millar Tip catheter and (D) determination of left atrial (LA) volume index assessed by magnetic resonance imaging in 38-week-old controls (Ctr; n=7), SHR-lean (n=7), and SHR-obese (n=7). All values are mean±SEM. $^{**}P<0.01$.

Discussion

This study demonstrates that concomitant obesity and MetS in hypertensive rats add to the development of an arrhythmogenic substrate in the atrium, increasing AF susceptibility. At 38 weeks of age, blood pressure was comparably increased in SHR-lean and SHR-obese. Obesity and insulin resistance in addition to hypertension in SHR-obese was associated with increased intramyocardial triglyceride content, enhanced extracellular matrix formation, increased myocyte diameters, and prolonged atrial refractoriness. As a result of these structural and electrophysiological changes, SHR-obese displayed local atrial conduction disturbances, increased AF susceptibility, and impaired regional and global LA emptying function parameters. These changes were less pronounced in SHR-lean.

To date, single cardiac risk factors such as hypertension, diabetes mellitus, obesity, and sleep apnea have been shown to independently lead to structural and electrical remodeling

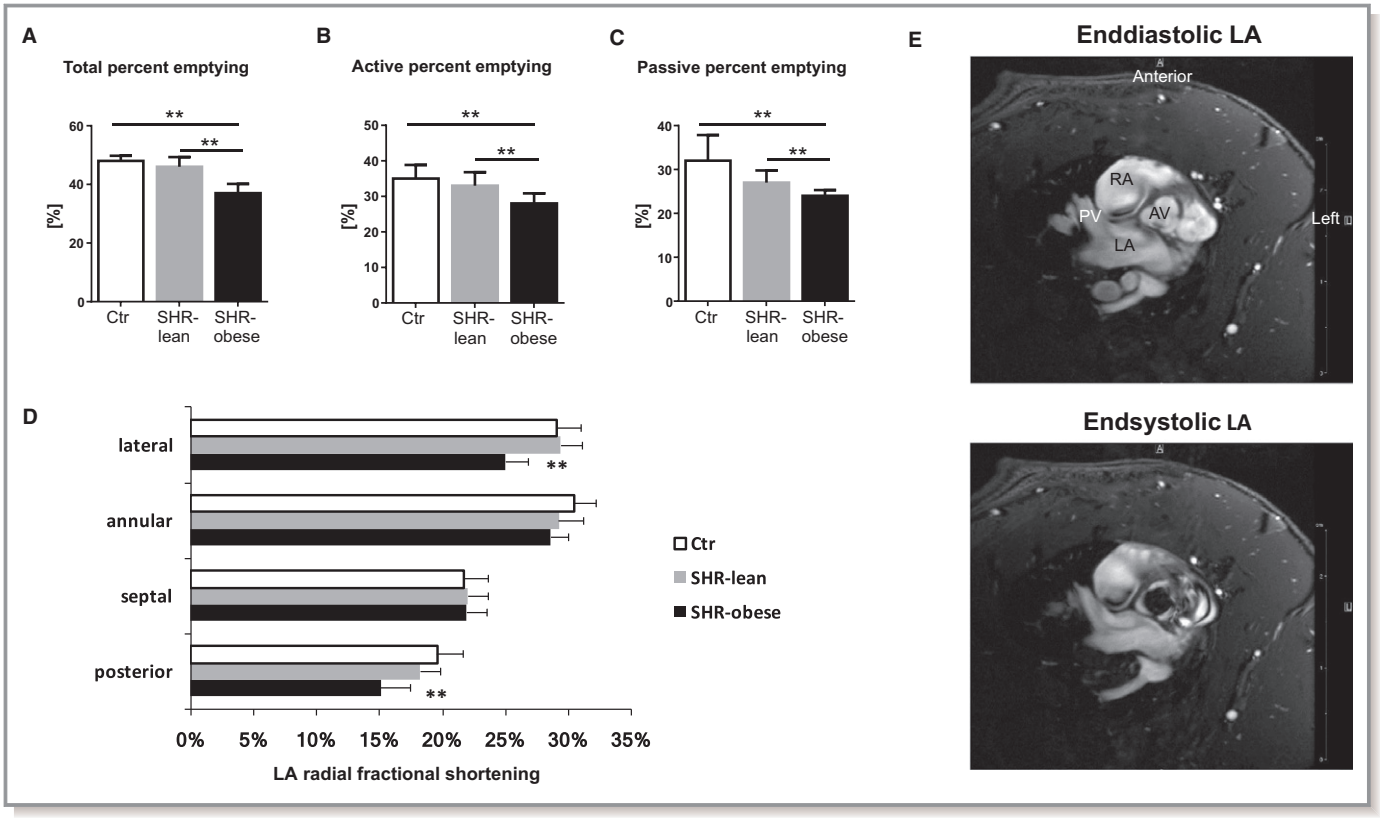

Figure 3. Emptying function of the left atrium (LA). Left atrial emptying function was assessed by magnetic resonance imaging in 7 animals per group. Quantification of global left atrial emptying function: (A) total percent emptying, (B) active percent emptying, and (C) passive percent emptying. Determination of regional left atrial wall motion: (D) lateral, annular, septal, and posterior radial fractional shortening of the LA. E, Representative MRI images of rat atria. AV indicates aortic valve; PV, pulmonary vein; RA, right atrium. All values are mean±SEM. $^{**}P<0.01$.

processes of the atria.[6–11] The clinical observation that the number of risk factors a patient with AF presents with is associated with progression of the arrhythmia suggests that at least certain combinations of risk factors may lead to more pronounced arrhythmogenic remodeling in the atrium.[3] In the present study, the evaluation of the additive effect of concomitant obesity and MetS in addition to hypertension by comparing SHR-obese with SHR-lean further supports this evidence.

Our study provides important insight into the impact of multiple concomitant risk factors on the atrial arrhythmogenic substrate. In SHR-obese, epicardial mapping revealed longer total atrial activation times and more areas of slower local atrial conduction when compared with both SHR-lean and controls. Local heterogeneities in conduction have been demonstrated to underlie the high AF susceptibility in structurally remodeled atria in a variety of animal models.[1,10,25,26] In addition, obesity appears to compound the effects of hypertension on extracellular matrix and endomysial fibrosis formation. In our model, there was an increase in myocyte-myocyte distances within bundles of the LA myocardium, for SHR-lean, and to a greater extent, for SHR-obese. However, total interstitial fibrosis formation was only increased in SHR-obese. An increase in endomysial fibrosis is consistent with changes observed in patients with AF and animal models for AF.[11,25–28] Despite enhanced visceral and subcutaneous adipose tissue in SHR-obese, we did not observe increased epicardial fat depots, as has been previously described in obese sheep models.[10] This observation suggests a different spatial fat distribution than large animals such as sheep and goats. Although we could not detect fatty dispositions in LA histological stainings, intramyocardial triglyceride content was increased in SHR-obese but not SHR-lean, compared with controls. There is emerging evidence that ectopic fat may have a significant and independent role in the development of AF.[29–31] The absence of fascial barriers between epicardial fat and the atrial musculature and the common vascular supply may facilitate paracrine action.[32,33] The documented structural atrial changes, particularly the increase in extracellular matrix and endomysial fibrosis formation, may result in disruption of side-to-side electrical connections between muscle bundles accounting for conduction abnormalities and increased AF susceptibility observed in SHR-obese compared with SHR-lean and controls. AERP was similarly prolonged in SHR-obese and SHR-lean. AERP prolongation has been reported in animal models for

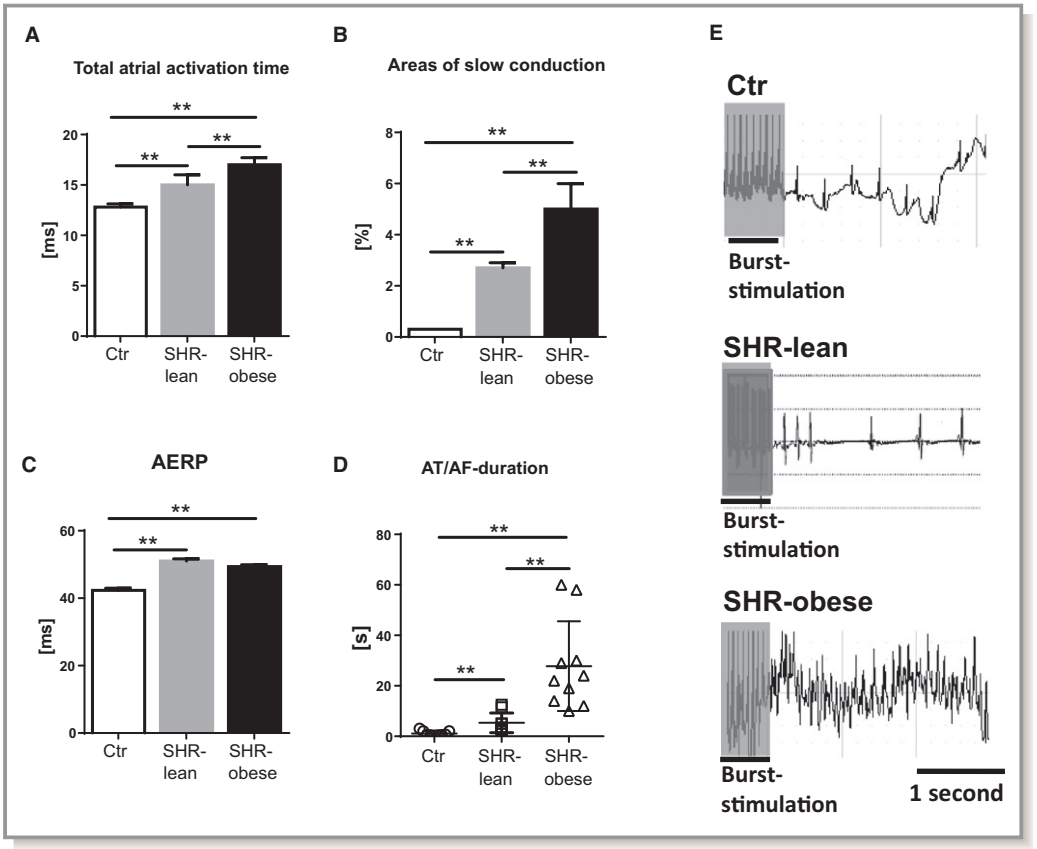

Figure 4. Atrial electrophysiological analysis and duration of burst-induced atrial fibrillation. Quantification of (A) global atrial activation time and (B) areas of slow conduction. C, Atrial effective refractory period (AERP) (n=10 per group). D, Duration of induced episodes of atrial fibrillation (AF) and (E) representative original traces of AF episodes. Ctr indicates controls; SHR-lean, lean spontaneously hypertensive rats; SHR-obese, obese spontaneously hypertensive rats. All values are mean±SEM. $^{**}P<0.01$.

congestive heart failure[26] and dilated atria[25] and there are reports of action potential prolongation leading to polymorphic atrial tachycardia that degenerates into AF.[1] Moreover, we found an impairment of regional and global LA emptying function in SHR-obese, which may be a functional consequence of the documented structural atrial changes together with moderate diastolic ventricular dysfunction in SHR-obese. In addition, expression of cardiac sarcoplasmic reticulum calcium ATPase type 2A was diminished in SHR-obese, indicating an impairment in cardiac calcium handling, which may contribute to the observed changes in global and regional LA emptying function in SHR-obese. Comparable changes in sarcoplasmic reticulum calcium ATPase type 2A expression were not detected in SHR-lean.

Telemetry showed a lower heart rate in SHR-lean and SHR-obese compared with controls, which was not observed with blood pressure measurements by the tail-cuff technique in a previous study.[21] These differences may be explained by restraining of rats and subsequent stress induction during tail-cuff experiments, which can be avoided by telemetry.

The development of an arrhythmogenic substrate in SHR-lean and SHR-obese came along with increased gene expression of the profibrotic cytokine TGF-β as well as increased expression of collagens and connective tissue growth factor. A comparable increase in TGF-β was previously observed in a sheep model with obesity.[10] In SHR-obese, but not in SHR-lean, LA gene expression as well as plasma concentrations of the profibrotic and proinflammatory pleiotropic adhesion protein OPN were significantly upregulated. OPN is a multifunctional cytokine[34] critically involved in cardiac fibrosis[16] and is upregulated in adipocytes, fibroblasts, and cardiomyocytes under several pathophysiological conditions including obesity and diabetes mellitus.[14] Modulation of immune cell response by OPN has been associated with adipose tissue inflammation and fibrotic remodeling of adipose tissue,[14] and this may be involved in the generation of an arrhtyhmogenic substrate.[35] Furthermore, OPN has been shown to be indispensable for angiotensin II and TGF-β–mediated fibrosis generation[36,37] and recombinant OPN enhances fibrosis in cardiac fibroblasts.[37] OPN deficiency exaggerates adverse LV remodeling in mice with myocardial

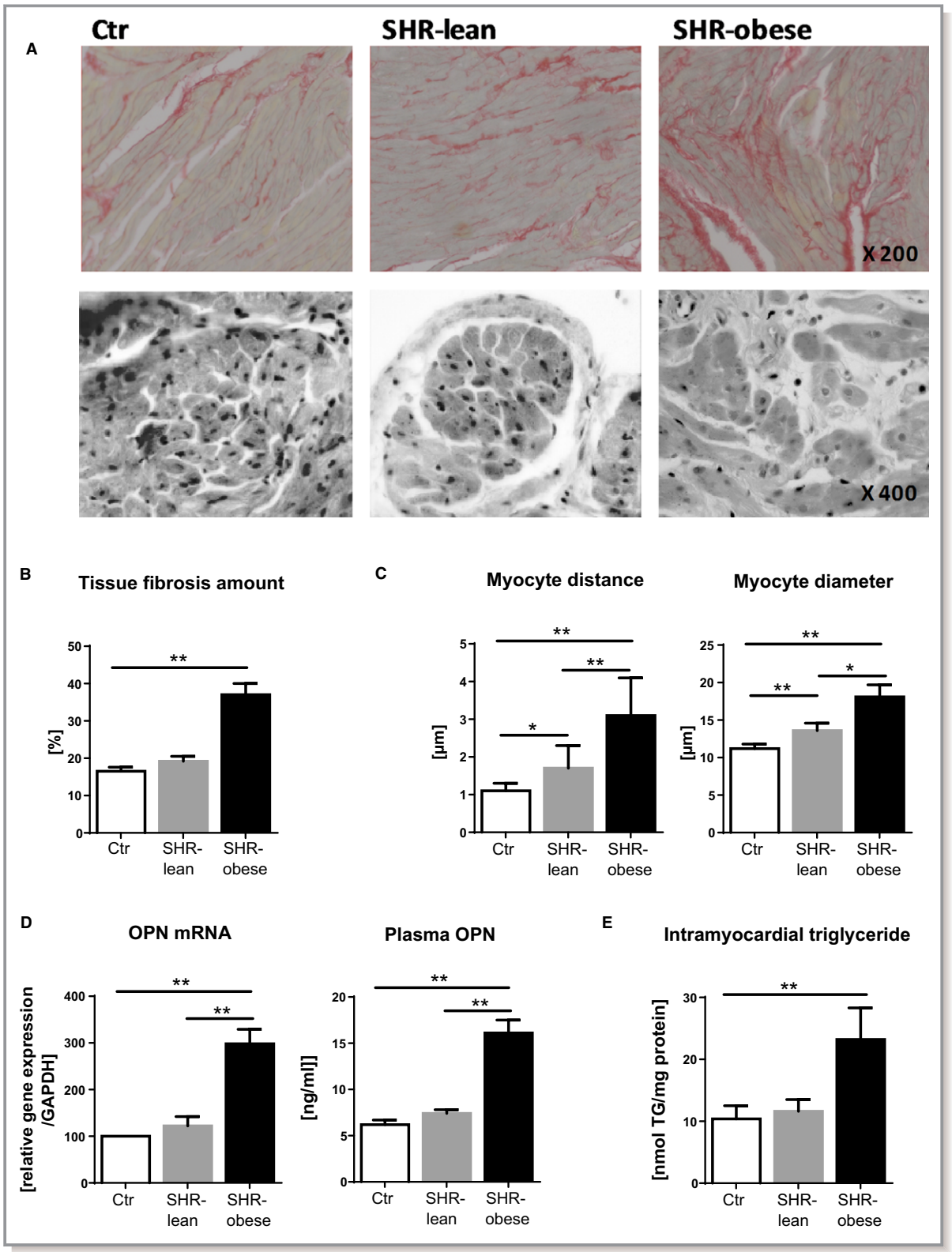

Figure 5. Atrial structural remodeling. A, Representative picture of Sirius red–stained atrium. B, Quantification of total atrial tissue fibrosis by Sirius red staining. C, Myocyte-myocyte distances within bundles as a measure of enhanced extracellular left atrial matrix formation and endomysial fibrosis formation and left atrial myocyte diameter. D, Gene expression analysis of osteopontin (OPN). Quantification of plasma OPN. E, Intramyocardial triglyceride content. Controls (Ctr; n=10), lean spontaneously hypertensive rats (SHR-lean) (n=10), and obese spontaneously hypertensive rats (SHR-obese) (n=10). All values are mean±SEM. **P*<0.05, ***P*<0.01.

Table. Differential Gene Expression in SHR-Lean and SHR-Obese Rat Controls (n=10), SHR-Lean (n=10), and SHR-Obese (n=10)

Relative Gene Expression/ GAPDH	Controls, %	SHR-Lean, %	SHR-Obese, %
TGF-β	100	127±11*	145±18†
CTGF	100	132±15	189±15†
Col1a1	100	123±12*	177±11†,‡
Serca2A	100	89±22	64±15†

Values for lean spontaneously hypertensive rats (SHR-lean) and obese spontaneously hypertensive rats (SHR-obese) are standardized to the control group. Col1a1 indicates collagen 1a; CTGF, connective tissue growth factor; TGF-β, transforming growth factor β; Serca2A, sarcoplasmic reticulum calcium ATPase type 2A.
*P<0.05 vs controls.
†P<0.01 vs controls.
‡P<0.01 vs SHR-lean.

infarction[38] and streptozotocin-induced diabetic cardiomyopathy[39] impairing collagen synthesis and accumulation. Interestingly, OPN expression in adipose tissue as well as circulating OPN levels are elevated in obese patients compared with lean individuals,[40] and weight loss after low-caloric diets reduces OPN blood levels in obese individuals.[39] Recent results showed that high blood OPN levels independently predicted AF recurrence in patients undergoing AF ablation.[18] Whether changes in OPN upon weight loss contribute to the antiarrhythmic effects documented in obese patients following weight reduction[41] and whether OPN provides a new therapeutic target to treat AF in obese patients warrants further research.

Herein, we provide an intensive characterization of the effects of concomitant obesity in a hypertensive rat model on atrial remodeling. Because of tissue size of the small rat atria, we had to focus on gene expression of some profibrotic markers and could not perform more detailed biochemical analysis within this study. In addition, SHR-lean and SHR-obese express hypertension and obesity for their genetic changes and some results from animal experiments cannot be directly extrapolated to humans but can be used to generate hypotheses for future research. Because of a large number of comparisons in this study, some statistically significant results may be attributable to chance alone.

In hypertensive rats, concomitant obesity and MetS add to the atrial arrhythmogenic phenotype by LV diastolic dysfunction, impaired regional and global LA emptying function, local conduction abnormalities, interstitial atrial fibrosis, and increased propensity for AF. This was associated with a pronounced upregulation of the profibrotic and proinflammatory adhesion protein OPN in SHR-obese but not in SHR-lean. SHR-obese may be a useful model to investigate mechanisms involved in the antiarrhythmic effects of interventions including weight loss in hypertension in the context of concomitant obesity and MetS.

Perspectives

In patients with hypertension and AF, aggressive blood pressure treatment alone did not improve ablation success compared with standard blood pressure treatment (SMAC-AF [Substrate Modification With Aggressive Blood Pressure Control] trial).[42] The findings of this study implicate the importance of clinical evaluation and management of concomitant risk factors such as obesity and MetS in patients with hypertension to maximize the prevention of the development of an atrial arrhythmogenic remodeling process and the progression of AF. Accordingly, aggressive risk factor and weight management improved the long-term success of AF ablation in patients with AF with a body mass index ≥27 kg/m^2 and ≥1 cardiac risk factor (ARREST-AF [Aggressive Risk Factor Reduction Study for Atrial Fibrillation and Implications for the Outcome of Ablation] study).[43] Given the lack of specific antifibrotic drugs available for clinical use, future research is warranted to determine the pathophysiological role of the proinflammatory adhesion protein OPN, which is upregulated in hypertension with concomitant obesity, and to test whether OPN may represent a pharmacological target to prevent atrial structural remodeling.

Acknowledgments

We thank Kathrin Gaspard and Jeannette Zimolong for their helpful support.

Sources of Funding

This work was funded by the German Society of Cardiology (DGK0914), the German Heart Foundation (F0315), the Else-Kröner-Fresenius Foundation (2014A306), and the German Research Foundation (KFO 196).

Disclosures

Dr Lau is supported by the Robert J. Craig Lectureship from the University of Adelaide. Dr Elliott is supported by a postdoctoral fellowship from the National Heart Foundation of Australia. Dr Mahajan is supported by an Early Career Fellowship from the National Health and Medical Research Council of Australia and National Heart Foundation and by the Leo J. Mahar Lectureship by the University of Adelaide. Dr Henriks is supported by an Early Career Fellowship from the National Heart Foundation of Australia and by the Derek Frewin Lectureship from the University of Adelaide. Dr Sanders is supported by Practitioner Fellowships from the

National Health and Medical Research Council of Australia and by the National Heart Foundation of Australia. Dr Linz is supported by a Beacon Research Fellowship from the University of Adelaide. Dr Mahajan reports having received lecture and/or consulting fees from St Jude Medical and Medtronic. Dr Mahajan reports having received research funding from St Jude Medical and Medtronic. Dr Sanders reports having received lecture and/or consulting fees from Biosense-Webster, Medtronic, St Jude Medical, and Boston Scientific. Dr Sanders reports having received research funding from Medtronic, St Jude Medical, Boston Scientific, Biotronik and Sorin.

References

1. Schotten U, Verheule S, Kirchhof P, Goette A. Pathophysiological mechanisms of atrial fibrillation: a translational appraisal. *Physiol Rev*. 2011;91:265–325.
2. Wijffels MC, Kirchhof CJ, Dorland R, Allessie MA. Atrial fibrillation begets atrial fibrillation. A study in awake chronically instrumented goats. *Circulation*. 1995;92:1954–1968.
3. Nabauer M, Gerth A, Limbourg T, Schneider S, Oeff M, Kirchhof P, Goette A, Lewalter T, Ravens U, Meinertz T, Breithardt G, Steinbeck G. The registry of the German Competence NETwork on Atrial Fibrillation: patient characteristics and initial management. *Europace*. 2009;11:423–434.
4. Schillaci G, Pirro M, Vaudo G, Gemelli F, Marchesi S, Porcellati C, Mannarino E. Prognostic value of the metabolic syndrome in essential hypertension. *J Am Coll Cardiol*. 2004;43:1817–1822.
5. Grossman W. Diastolic dysfunction in congestive heart failure. *N Engl J Med*. 1991;325:1557–1564.
6. Lau DH, Shipp NJ, Kelly DJ, Thanigaimani S, Neo M, Kuklik P, Lim HS, Zhang Y, Drury K, Wong CX, Chia NH, Brooks AG, Dimitri H, Saint DA, Brown L, Sanders P. Atrial arrhythmia in ageing spontaneously hypertensive rats: unraveling the substrate in hypertension and ageing. *PLoS One*. 2013;8:e72416.
7. Diness JG, Skibsbye L, Jespersen T, Bartels ED, Sørensen US, Hansen RS, Grunnet M. Effects on atrial fibrillation in aged hypertensive rats by Ca(2+)-activated K(+) channel inhibition. *Hypertension*. 2011;57:1129–1135.
8. Lau DH, Mackenzie L, Kelly DJ, Psaltis PJ, Worthington M, Rajendram A, Kelly DR, Nelson AJ, Zhang Y, Kuklik P, Brooks AG, Worthley SG, Faull RJ, Rao M, Edwards J, Saint DA, Sanders P. Short-term hypertension is associated with the development of atrial fibrillation substrate: a study in an ovine hypertensive model. *Heart Rhythm*. 2010;7:396–404.
9. Lau DH, Mackenzie L, Kelly DJ, Psaltis PJ, Brooks AG, Worthington M, Rajendram A, Kelly DR, Zhang Y, Kuklik P, Nelson AJ, Wong CX, Worthley SG, Rao M, Faull RJ, Edwards J, Saint DA, Sanders P. Hypertension and atrial fibrillation: evidence of progressive atrial remodeling with electrostructural correlate in a conscious chronically instrumented ovine model. *Heart Rhythm*. 2010;7:1282–1290.
10. Mahajan R, Lau DH, Brooks AG, Shipp NJ, Manavis J, Wood JP, Finnie JW, Samuel CS, Royce SG, Twomey DJ, Thanigaimani S, Kalman JM, Sanders P. Electrophysiological, electroanatomical, and structural remodeling of the atria as consequences of sustained obesity. *J Am Coll Cardiol*. 2015;66:1–11.
11. Linz D, Hohl M, Dhein S, Ruf S, Reil JC, Kabiri M, Wohlfart P, Verheule S, Böhm M, Sadowski T, Schotten U. Cathepsin A mediates susceptibility to atrial tachyarrhythmia and impairment of atrial emptying function in Zucker diabetic fatty rats. *Cardiovasc Res*. 2016;110:371–380.
12. Nattel S. New ideas about atrial fibrillation 50 years on. *Nature*. 2002;415:219–226.
13. Jalife J, Kaur K. Atrial remodeling, fibrosis, and atrial fibrillation. *Trends Cardiovasc Med*. 2015;25:475–484.
14. Kahles F, Findeisen HM, Bruemmer D. Osteopontin: a novel regulator at the cross roads of inflammation, obesity and diabetes. *Mol Metab*. 2014;3:384–393.
15. Matsui Y, Jia N, Okamoto H, Kon S, Onozuka H, Akino M, Liu L, Morimoto J, Rittling SR, Denhardt D, Kitabatake A, Uede T. Role of osteopontin in cardiac fibrosis and remodeling in angiotensin II-induced cardiac hypertrophy. *Hypertension*. 2004;43:1195–1201.
16. Lenga Y, Koh A, Perera AS, McCulloch CA, Sodek J, Zohar R. Osteopontin expression is required for myofibroblast differentiation. *Circ Res*. 2008;102:319–327.
17. Wu CH, Hu YF, Chou CY, Lin YJ, Chang SL, Lo LW, Tuan TC, Li CH, Chao TF, Chung FP, Liao JN, Chen SA. Transforming growth factor-β1 level and outcome after catheter ablation for nonparoxysmal atrial fibrillation. *Heart Rhythm*. 2013;10:10–15.
18. Güneş HM, Babur Güler G, Güler E, Demir GG, Kızılırmak Yılmaz F, Omaygenç MO, İstanbullu Tosun A, Akgün T, Boztosun B, Kılıçarslan F. Relationship between serum osteopontin level and atrial fibrillation recurrence in patients undergoing cryoballoon catheter ablation. *Turk Kardiyol Dern Ars*. 2017;45:26–32.
19. Ernsberger P, Koletsky RJ, Friedman JE. Molecular pathology in the obese spontaneous hypertensive Koletsky rat: a model of syndrome X. *Ann N Y Acad Sci*. 1999;892:272–288.
20. Linz D, Hohl M, Mahfoud F, Reil JC, Linz W, Hübschle T, Juretschke HP, Neumann-Häflin C, Rütten H, Böhm M. Cardiac remodeling and myocardial dysfunction in obese spontaneously hypertensive rats. *J Transl Med*. 2012;10:187.
21. Linz B, Hohl M, Reil JC, Böhm M, Linz D. Inhibition of NHE3-mediated sodium absorption in the gut reduced cardiac end-organ damage without deteriorating renal function in obese spontaneously hypertensive rats. *J Cardiovasc Pharmacol*. 2016;67:225–231.
22. Linz D, Wirth K, Linz W, Heuer HO, Frick W, Hofmeister A, Heinelt U, Arndt P, Schwahn U, Böhm M, Ruetten H. Antihypertensive and laxative effects by pharmacological inhibition of sodium-proton-exchanger subtype 3-mediated sodium absorption in the gut. *Hypertension*. 2012;60:1560–1567.
23. Jarvinen V, Kupari M, Hekali P, Poutanen VP. Assessment of left atrial volumes and phasic function using cine magnetic resonance imaging in normal subjects. *Am J Cardiol*. 1994;73:1135–1138.
24. Nori D, Raff G, Gupta V, Gentry R, Boura J, Haines DE. Cardiac magnetic resonance imaging assessment of regional and global left atrial function before and after catheter ablation for atrial fibrillation. *J Interv Card Electrophysiol*. 2009;26:109–117.
25. Neuberger HR, Schotten U, Verheule S, Eijsbouts S, Blaauw Y, van Hunnik A, Allessie M. Development of a substrate of atrial fibrillation during chronic atrioventricular block in the goat. *Circulation*. 2005;111:30–37.
26. Li D, Fareh S, Leung TK, Nattel S. Promotion of atrial fibrillation by heart failure in dogs: atrial remodeling of a different sort. *Circulation*. 1999;100:87–95.
27. Verheule S, Wilson E, Everett TT, Shanbhag S, Golden C, Olgin J. Alterations in atrial electrophysiology and tissue structure in a canine model of chronic atrial dilatation due to mitral regurgitation. *Circulation*. 2003;107:2615–2622.
28. Verheule S, Tuyls E, Gharaviri A, Hulsmans S, van Hunnik A, Kuiper M, Serroyen J, Zeemering S, Kuijpers NH, Schotten U. Loss of continuity in the thin epicardial layer because of endomysial fibrosis increases the complexity of atrial fibrillatory conduction. *Circ Arrhythm Electrophysiol*. 2013;6:202–211.
29. Hatem SN, Redheuil A, Gandjbakhch E. Cardiac adipose tissue and atrial fibrillation: the perils of adiposity. *Cardiovasc Res*. 2016;109:502–509.
30. Thanassoulis G, Massaro JM, O'Donnell CJ, Hoffmann U, Levy D, Ellinor PT, Wang TJ, Schnabel RB, Vasan RS, Fox CS, Benjamin EJ. Pericardial fat is associated with prevalent atrial fibrillation: the Framingham Heart Study. *Circ Arrhythm Electrophysiol*. 2010;3:345–350.
31. Wong CX, Abed HS, Molaee P, Nelson AJ, Brooks AG, Sharma G, Leong DP, Lau DH, Middeldorp ME, Roberts-Thomson KC, Wittert GA, Abhayaratna WP, Worthley SG, Sanders P. Pericardial fat is associated with atrial fibrillation severity and ablation outcome. *J Am Coll Cardiol*. 2011;57:1745–1751.
32. Venteclef N, Guglielmi V, Balse E, Gaborit B, Cotillard A, Atassi F, Amour J, Leprince P, Dutour A, Clément K, Hatem SN. Human epicardial adipose tissue induces fibrosis of the atrial myocardium through the secretion of adipo-fibrokines. *Eur Heart J*. 2015;36:795–805.
33. Spach MS, Boineau JP. Microfibrosis produces electrical load variations due to loss of side-to-side cell connections: a major mechanism of structural heart disease arrhythmias. *Pacing Clin Electrophysiol*. 1997;20:397–413.
34. Mazzali M, Kipari T, Ophascharoensuk V, Wesson JA, Johnson R, Hughes J. Osteopontin—a molecule for all seasons. *QJM*. 2002;95:3–13.
35. Haemers P, Hamdi H, Guedj K, Suffee N, Farahmand P, Popovic N, Claus P, LePrince P, Nicoletti A, Jalife J, Wolke C, Lendeckel U, Jaïs P, Willems R, Hatem SN. Atrial fibrillation is associated with the fibrotic remodelling of adipose tissue in the subepicardium of human and sheep atria. *Eur Heart J*. 2017;38:53–61.
36. Lorenzen JM, Schauerte C, Hübner A, Kölling M, Martino F, Scherf K, Batkai S, Zimmer K, Foinquinos A, Kaucsar T, Fiedler J, Kumarswamy R, Bang C, Hartmann D, Gupta SK, Kielstein J, Jungmann A, Katus HA, Weidemann F, Müller OJ, Haller H, Thum T. Osteopontin is indispensible for AP1-mediated angiotensin II-related miR-21 transcription during cardiac fibrosis. *Eur Heart J*. 2015;36:2184–2196.
37. Ashizawa N, Graf K, Do YS, Nunohiro T, Giachelli CM, Meehan WP, Tuan TL, Hsueh WA. Osteopontin is produced by rat cardiac fibroblasts and mediates A (II)-induced DNA synthesis and collagen gel contraction. *J Clin Invest*. 1996;98:2218–2227.

38. Trueblood NA, Xie Z, Communal C, Sam F, Ngoy S, Liaw L, Jenkins AW, Wang J, Sawyer DB, Bing OH, Apstein CS, Colucci WS, Singh K. Exaggerated left ventricular dilation and reduced collagen deposition after myocardial infarction in mice lacking osteopontin. *Circ Res*. 2001;88:1080–1087.

39. Subramanian V, Krishnamurthy P, Singh K, Singh M. Lack of osteopontin improves cardiac function in streptozotocin-induced diabetic mice. *Am J Physiol Heart Circ Physiol*. 2007;292:H673–H683.

40. Gómez-Ambrosi J, Catalán V, Ramírez B, Rodríguez A, Colina I, Silva C, Rotellar F, Mugueta C, Gil MJ, Cienfuegos JA, Salvador J, Frühbeck G. Plasma osteopontin levels and expression in adipose tissue are increased in obesity. *J Clin Endocrinol Metab*. 2007;92:3719–3727.

41. Pathak RK, Middeldorp ME, Meredith M, Mehta AB, Mahajan R, Wong CX, Twomey D, Elliott AD, Kalman JM, Abhayaratna WP, Lau DH, Sanders P. Long-term effect of goal-directed weight management in an atrial fibrillation cohort: a long-term follow-up study (LEGACY). *J Am Coll Cardiol*. 2015;65:2159–2169.

42. Parkash R, Wells GA, Sapp JL, Healey JS, Tardif JC, Greiss I, Rivard L, Roux JF, Gula L, Nault I, Novak PG, Birnie DH, Ha AC, Wilton SB, Mangat I, Gray CJ, Gardner MJ, Tang AS. The effect of aggressive blood pressure control on the recurrence of atrial fibrillation after catheter ablation: a randomized, open label, clinical trial (Substrate Modification with Aggressive Blood Pressure Control: SMAC-AF). *Circulation*. 2017;135:1788–1798.

43. Pathak RK, Middeldorp ME, Lau DH, Mehta AB, Mahajan R, Twomey D, Alasady M, Hanley L, Antic NA, McEvoy RD, Kalman JM, Abhayaratna WP, Sanders P. Aggressive risk factor reduction study for atrial fibrillation and implications for the outcome of ablation: the ARREST-AF cohort study. *J Am Coll Cardiol*. 2014;64:2222–2231.